Current Biology, Vol. 15, 1755–1761, October 11, 2005, ©2005 Elsevier Ltd All rights reserved. DOI 10.1016/j.cub.2005.08.049

Xnf7 Contributes to Spindle Integrity through Its Microtubule-Bundling Activity

Thomas J. Maresca, Hanspeter Niederstrasser, Karsten Weis, and Rebecca Heald*
Department of Molecular and Cell Biology
University of California, Berkeley
Berkeley, California 94720-3200

Summary

Regulation of microtubule dynamics and organization in mitosis by a number of microtubule-associated proteins (MAPs) is required for proper bipolar spindle assembly, yet the precise mechanisms by which many MAPs function are poorly understood [1]. One interesting class of MAPs is known to localize to the nucleus during interphase yet fulfill important spindle functions during mitosis. We have identified *Xenopus* nuclear factor 7 (Xnf7), a developmental regulator of dorsal-ventral patterning [2, 3], as a microtubule-binding protein that also associates with the nuclear import receptor importin α/β. Xnf7 localized to interphase nuclei and metaphase spindles both in *Xenopus* egg extracts and cultured cells. Xnf7-depleted spindles were hypersensitive to microtubule-depolymerizing agents. Functional characterization of Xnf7 revealed that it binds directly to microtubules, exhibits RING-finger-dependent E3-ubiquitin-ligase activity, and has C-terminal-dependent microtubule-bundling activity. The minimal microtubule-bundling domain of Xnf7 was sufficient to rescue the spindle-hypersensitivity phenotype. Thus, we have identified Xnf7 as a nuclear MAP whose microtubule-bundling activity, but not E3-ligase activity, contributes to microtubule organization and spindle integrity. Characterization of the multiple activities of Xnf7 may have implications for understanding human diseases caused by mutations in related proteins.

Results

Biochemical Identification of Xnf7 as a Microtubule-Associated Importin β Cargo

A number of microtubule-associated proteins (MAPs) have been shown to localize to the spindle during mitosis and to the nucleus during interphase [4, 5]. MAPs that exhibit this localization pattern are candidates for regulation by Ran and import receptors. To identify potential importin β-regulated MAPs, we performed complimentary affinity-chromatography-based purifications. First, MAPs from metaphase cytostatic factor (CSF)-arrested *Xenopus laevis* egg extract were isolated and subsequently subjected to an importin β column to enrich for potential cargoes (Figure 1A). Reciprocally, importin β cargoes were isolated from extract and incubated with pure taxol-stabilized microtubules to identify those that behaved as MAPs (Figure 1B). These complimentary biochemical purifications both yielded a prominent common band at ~78 kDa that was identified as Xnf7 by microsequencing. Pulldowns were performed with purified components to demonstrate that the nuclear localization signal (NLS) of Xnf7 mediates binding of Xnf7 to importin β via the adaptor protein importin α in a RanGTP reversible manner (see Figure S1 in the Supplemental Data available with this article online).

Xnf7 was previously identified as a regulator of dorsal-ventral patterning in the *Xenopus* embryo [2, 3]. Nuclear accumulation of Xnf7 requires a bipartite NLS that has been mapped to amino acids 31–127 (Figure 1C) [6]. In addition, Xnf7 contains an N-terminal CHROMO domain (aa 31–91), a C3HC4-type RING finger (aa 145–184), a B-box (aa 219–260), a leucine-rich coiled coil (aa 270–393), and a C-terminal PRY/SPRY domain (aa 431–609) (Figure 1C). The conserved arrangement of its RING-finger, B-box, and coiled-coil domains identifies Xnf7 as a *tri*partite *mo*tif (TRIM) family member [7, 8].

Xnf7 Localizes to Interphase Nuclei and Mitotic Spindles in *Xenopus* Extract and Cultured Cells

In order to further characterize Xnf7 localization and function, we generated a polyclonal antibody against recombinant Xnf7 that detected a single band at 78 kDa by western blot of egg extracts (Figure 1D) and specifically immunoprecipitated Xnf7 as determined by mass spectrometry (data not shown). By immunofluorescence analysis, we determined that Xnf7 localized to spindles assembled in metaphase extract and was nuclear during interphase (Figure 1E), a pattern similar to that observed in post-mid-blastula transition (MBT) *X. laevis* embryos [9, 10]. Interestingly, the phosphorylation-dependent cytoplasmic-retention mechanism that prevents nuclear localization of Xnf7 in the early embryo appears to be absent from the extract system, perhaps as a result of differing phosphorylation states and/or lack of a cell cortex. A similar localization pattern was also observed in cultured *Xenopus* cells (Figure S2). Notably, Xnf7 localized to discrete and punctate nuclear bodies in interphase cells. PwA33, a *Pleurodeles waltl* ortholog of Xnf7, has been proposed to associate with an RNP matrix [11, 12]; however, the nature and composition of the Xnf7 nuclear bodies is currently unknown.

Xnf7-Depleted Spindles Are More Sensitive to Microtubule Depolymerization

In order to investigate the function of Xnf7 in spindle assembly, we used the polyclonal antibody to deplete greater than 95% of the protein from egg extracts as determined by western-blot analysis (Figure 2A). Xnf7-depleted extracts supported the assembly of spindles with normal morphology around sperm nuclei or chromatin beads when compared to mock-depleted reactions (Figure 2B). To examine whether the structural integrity of the spindle was nevertheless compromised, we challenged mock- and Xnf7-depleted spindles with microtubule-destabilizing factors. The addition of Op18/Stathmin, a microtubule catastrophe-inducing factor, to

*Correspondence: heald@socrates.berkeley.edu

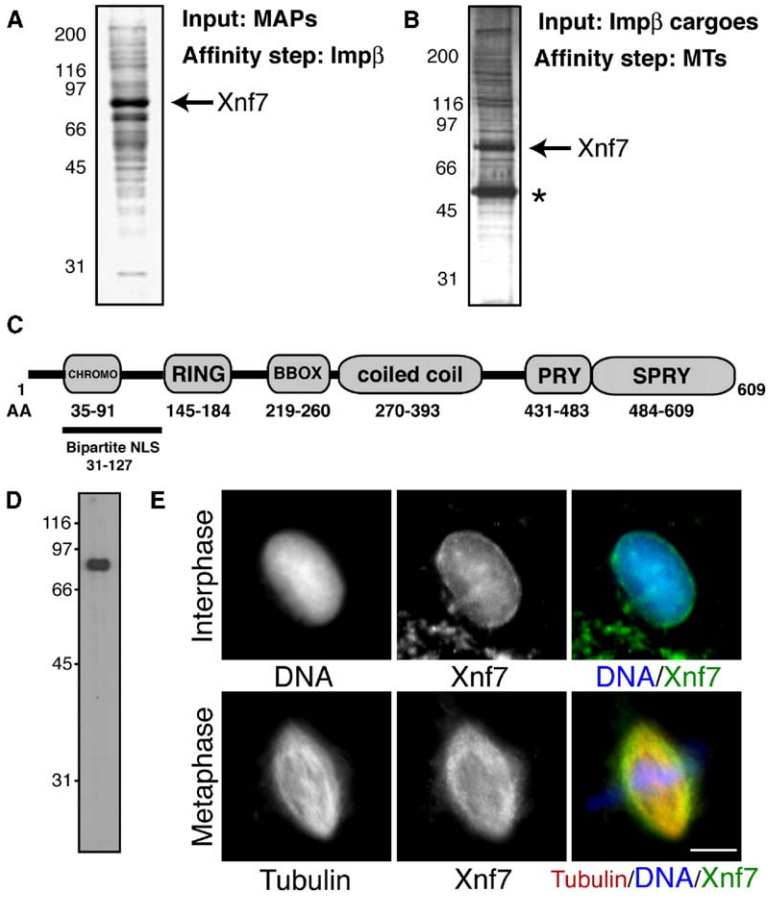

Figure 1. Biochemical Identification of Xnf7 and Its Localization in *Xenopus* Egg Extracts

(A) Mitotic MAPs, purified from *Xenopus* egg extract, were incubated with an importin β matrix, eluted, and subjected to SDS-PAGE before Coomassie staining. The arrow points to the abundant 78 kDa MAP that was identified as Xnf7 by microsequencing.

(B) Importin β cargoes were purified from *Xenopus* egg extracts, eluted, and incubated with taxol-stabilized microtubules before pelleting through a sucrose cushion. The microtubule-associated cargoes were then eluted, subjected to SDS-PAGE, and silver stained. The most abundant band after tubulin (asterisk) was the 78 kDa protein Xnf7 (arrow).

(C) Schematic representation of the domain structure of Xnf7.

(D) The affinity-purified Xnf7 antibody recognizes one 78 kDa band by western-blot analysis of total egg extract.

(E) Immunolocalization of Xnf7 in interphase (top) and metaphase (bottom) extracts. Nuclei were stained for DNA (blue) and Xnf7 (green). Xnf7 localizes to spindles assembled in metaphase-arrested extract. In the merged metaphase image, microtubules are red, DNA is blue, and Xnf7 is green. The scale bar = 10 μm.

approximately 1.5 times its endogenous concentration caused the shortening and collapse of Xnf7-depleted spindles but had little effect on control spindle morphology (Figure 2C) [13–15]. Similarly, titration experiments with the microtubule-depolymerizing drug nocodazole revealed that Xnf7-depleted spindles were more sensitive to the drug and collapsed and/or lost bipolarity at concentrations (10 and 50 ng/ml) that had minimal effects on control spindles (Figure 2D). Thus, Xnf7 function appears to contribute to the overall structural integrity of the spindle apparatus.

Xnf7 Binds to and Bundles Microtubules in vitro

Having observed that Xnf7 interacts with microtubules in extracts and tissue-culture cells (Figure 1 and Figure S2) and contributes to spindle integrity, we sought to determine whether Xnf7 could affect microtubule polymerization and organization directly. Purified Xnf7 cosedimented with microtubules at tubulin concentrations equal to or above 0.5 μM (Figure 3A), indicating that Xnf7 binds directly and specifically to microtubules in vitro [4, 16].

Xnf7 did not appear to affect the polymerization of pure tubulin in vitro (data not shown). However, we found that taxol-stabilized microtubules became organized into large bundled arrays in the presence of Xnf7 at concentrations greater than ~0.5–0.75 μM in a dose-dependent manner (Figure 3B). The structures were negatively stained and viewed by electron microscopy to confirm that they were indeed bundled microtubules. Whereas control conditions contained individual microtubule polymers, in the presence of Xnf7 we observed bundled arrays often consisting of greater than ten aligned microtubules (Figure 3C). Importin α/β binding did not significantly affect the microtubule binding or bundling by Xnf7, indicating that these activities are not regulated by the importin/RanGTP pathway (Figure S3).

For monitoring the kinetics of the Xnf7-mediated microtubule bundling, flow cells containing fluorescently labeled taxol-stabilized microtubules were assembled and imaged by time-lapse fluorescence microscopy as Xnf7 was introduced. A stable network of microtubule bundles formed within several seconds of introducing Xnf7 (Figure 3D and Movie S1). These bundles were extremely stable and did not dissociate over the course of several hours (data not shown). To investigate how such stable Xnf7-cross linked microtubule bundles would behave in the presence of microtubule-based motor activity, we employed a motility assay with conventional kinesin (Kinesin 1). Xnf7-generated microtubule bundles rapidly split apart into smaller structures that were transported away by immobilized motors (Movie S2). When bundles consisting of Alexa 488-labeled (green) and X-rhodamine-labeled (red) microtubules were utilized in the assay, we observed bundles split-

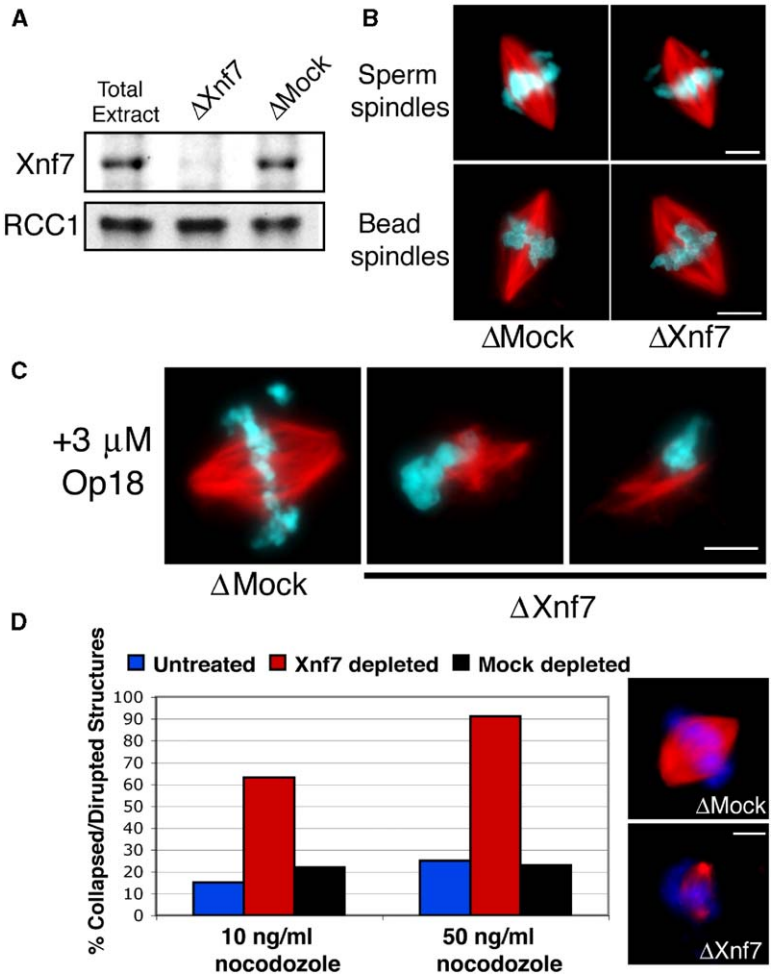

Figure 2. Xnf7-Depleted Spindles Are More Sensitive to Microtubule Depolymerization

(A) Western blot of total, Xnf7-depleted, and mock-depleted extract probed with Xnf7 antibodies to show that >95% of Xnf7 was removed from the extract whereas the control protein (RCC1) was unaffected by the depletion.

(B) Both sperm spindles and chromatin-bead spindles assembled normally in Xnf7-depleted extracts. Tubulin is shown in red and DNA in blue. Scale bars = 10 μm.

(C) Addition of low levels (~3 μM) of the catastrophe factor Op18 to extracts had little effect on the morphology of mock-depleted spindles but induced Xnf7-depleted spindles to collapse and/or become less organized. Tubulin is red and DNA is blue. The scale bar = 10 μm.

(D) A representative nocodazole titration experiment highlighting that low levels (10 and 50 ng/ml) of the microtubule depolymerizer had a more dramatic effect on Xnf7-depleted spindles compared to spindles assembled in either mock-depleted or untreated extracts. N = 100 structures for each condition. Representative examples of spindles from control and Xnf7-depleted reactions are shown next to the graph with tubulin in red and DNA in blue. The scale bar = 10 μm.

ting apart into smaller mobile structures consisting of both green and red microtubules (Movie S3). Thus, Xnf7-mediated microtubule bundles, although extremely stable in the absence of applied forces, are readily converted into motile, nonstatic structures upon interaction with motor proteins.

The Coiled Coil and SPRY Domains of Xnf7 Are Required for Its Microtubule-Binding and -Bundling Activities

Consistent with recently published results, we found that, in addition to its microtubule-bundling function, Xnf7 also exhibited RING-finger-dependent ubiquitin-E3-ligase activity in vitro (Figure 4A and Figure S4). A series of Xnf7 truncation mutants were constructed to identify which domains were essential for its functions. Xnf7 lacking the SPRY domain failed to bundle pure microtubules and also appeared to act in a dominant-negative fashion by inhibiting the bundling activity of Xnf7 in vitro, perhaps by sequestering Xnf7 into inactive aggregates (Figure S5). Other C-terminal truncations including $Xnf7^{1–265}$, $Xnf7^{1–218}$, and $Xnf7^{1–141}$ all failed to bind or bundle microtubules (Figure 4A). By constructing several N-terminal truncations, we were able to define $Xnf7^{265–609}$, consisting of the coiled coil (a reported homo-oligomerization domain [17]) and SPRY domains, as the minimal microtubule-binding and -bundling domain of Xnf7 (Figures 4A and 4B). Similar observations were reported for the related microtubule-bundling protein Mir1 [18].

Interestingly, addition of exogenous $Xnf7^{1–432}$ lacking the PRY/SPRY domain to extracts during spindle-assembly reactions resulted in aberrant and poorly organized microtubule structures containing large clumps of Xnf7 (Figure 4C). The effect of this truncation is notable because mutations in the SPRY domain of other TRIM family members are linked to a number of human diseases [19]. For example, loss of the SPRY domain in the microtubule-associated TRIM family member MID1 induces cytoplasmic aggregation of the protein and causes the human developmental disorder Opitz syndrome (OS) [20–22].

The Bundling Activity of Xnf7, Not Its E3-Ligase Activity, Contributes to Spindle Integrity

The nocodazole sensitivity of Xnf7-depleted spindles could be rescued by the addition of full-length recombinant Xnf7 to depleted extract at estimated endogenous levels (~3 μM), indicating that Xnf7 was the relevant activity being immunodepleted (Figures 4D and 4E).

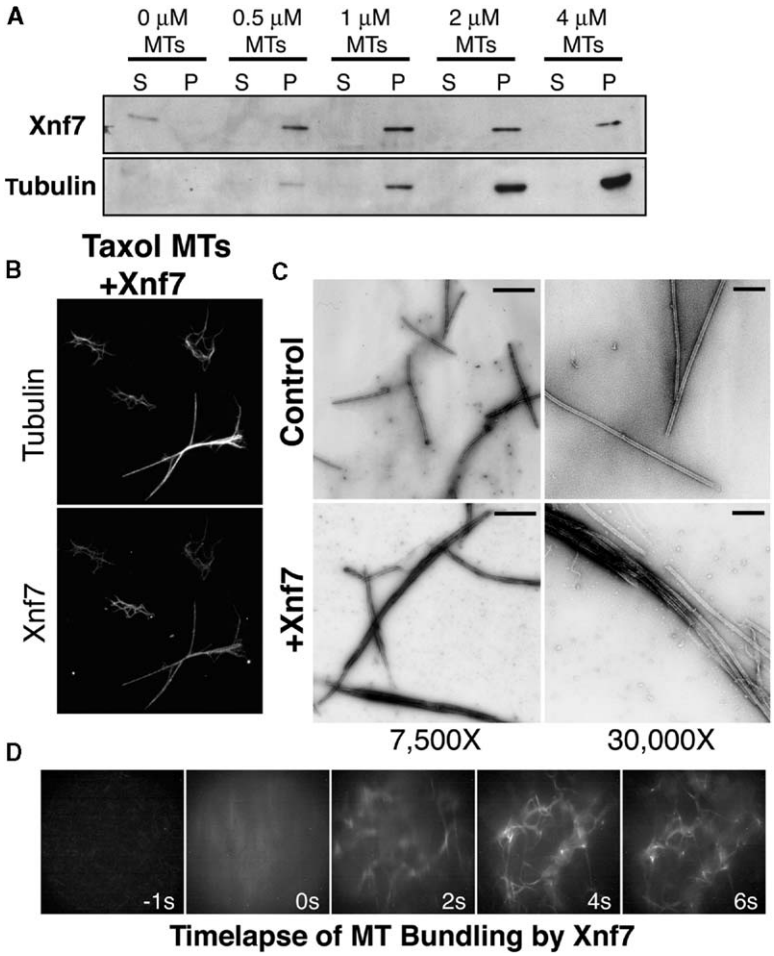

Figure 3. Xnf7 Binds Directly to Microtubules and Organizes Them into Bundled Arrays

(A) Microtubule cosedimentation analysis with the indicated concentrations of taxol-stabilized microtubules in the presence of 0.25 μM Xnf7. Equal loads of the supernatants (S) and pellets (P) from each microtubule concentration were blotted for Xnf7 (top panel) and tubulin (bottom panel). Xnf7 cosedimented with microtubules at concentrations equal to or above 0.5 μM.

(B) Taxol-stabilized microtubules are bundled by recombinant Xnf7. Two micromolar Xnf7 was incubated with 1 μM rhodamine-labeled taxol-stabilized microtubules, and the reactions were spun down and stained for Xnf7 by immunofluorescence. Microtubule bundles were detected at Xnf7 concentrations above ~0.75 μM. The scale bar = 10 μm.

(C) Structures were assembled in the presence of 2 μM Xnf7 before being imaged by electron microscopy to confirm that microtubules were indeed bundled. In the presence of Xnf7, large microtubule bundles were detected, whereas in control reactions, only individual microtubules were observed. The 7,500× scale bar = 1 μm; the 30,000× scale bar = 200 nm.

(D) A flow cell was filled with taxol-stabilized microtubules and imaged as Xnf7 was added to the chamber. A stable network of bundled microtubules assembled within ~2 s of introducing Xnf7. See Movie S1.

Utilizing the various Xnf7 truncations and point mutants that we had generated, we next investigated which functional domains of Xnf7 were required for spindle integrity. The nocodazole hypersensitivity of Xnf7-depleted spindles was fully rescued by adding back the minimal microtubule-bundling domain of Xnf7 ($Xnf7^{265–609}$), which lacks E3-ligase activity (Figures 4A, 4D, and 4E). These data strongly indicate that loss of Xnf7's microtubule-bundling activity rather than its E3-ligase activity is responsible for the hypersensitivity of Xnf7-depleted spindles to depolymerizing agents. Thus, Xnf7 contributes to the structural integrity of the spindle by bundling microtubules.

Discussion

Microtubule Bundles and the Spindle

In addition to individual microtubule polymers, the mitotic spindle consists of subpopulations of differentially bundled microtubules. For proper spindle structure and function, MAPs and motor proteins must act in the context of these bundled arrays to stabilize, destabilize, transport, and move along microtubules. Examining how MAPs and motors behave in the context of bundled fibers may further our understanding of what is happening in the complex spindle environment. For example, how might a processive directional motor move along a bundle of antiparallel microtubules? Also, how might microtubule destabilizers such as MCAK and Op18 act on a bundle of microtubules like a kinetochore fiber? The application of in vitro assays with bundled microtubules could help address these questions.

Stable, Xnf7 cross-linked microtubule bundles within the spindle could contribute to integrity and morphology by physically buttressing the structure. However, the stable Xnf7-mediated microtubule bundles can also transition into a dynamic and fluid state upon force application by molecular motors. Thus, bundling factors may generate microtubule arrays that impart structural stability to the spindle while simultaneously retaining critical dynamic properties when necessary.

RanGTP and importins do not appear to regulate the microtubule-binding and -bundling activity of Xnf7 during mitosis despite the fact that it is a nuclear cargo. It is possible that other activities of Xnf7 are regulated by the Ran pathway, or that the regulation exists purely at the level of localization, because nuclear transport could function to sequester Xnf7 away from microtubules. At the least, regulation of Xnf7 by import receptors likely serves an important developmental function because it is known that the localization pattern of Xnf7 is regulated during embryogenesis [2].

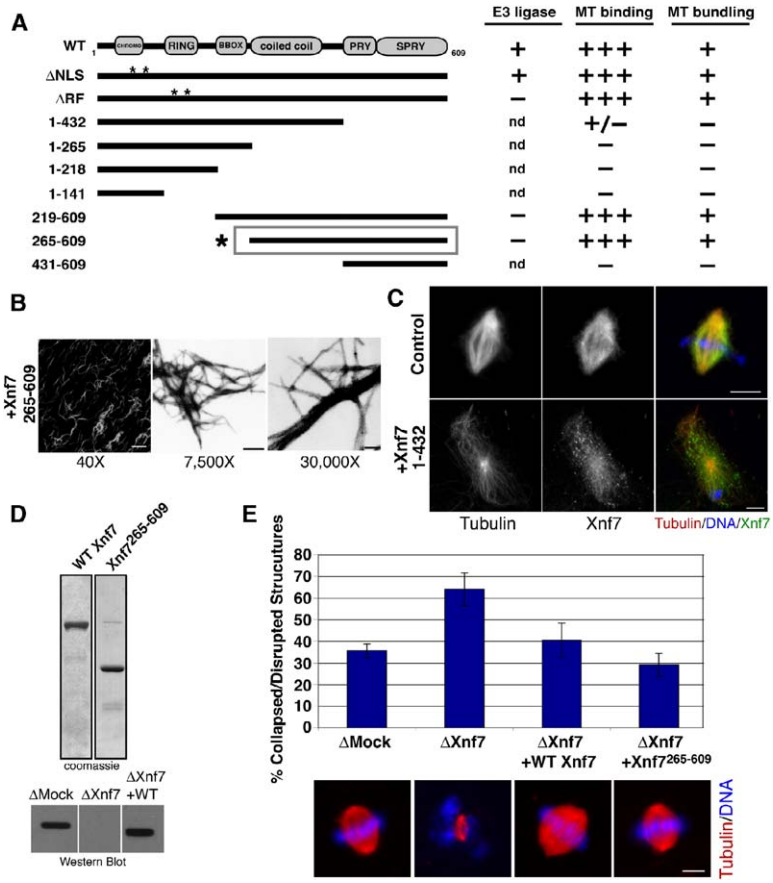

Figure 4. Functional Dissection of Xnf7 Reveals that Its Minimal Microtubule-Bundling Domain Is Sufficient to Rescue Spindle Hypersensitivity Caused by Xnf7 Depletion

(A) Schematic of the various Xnf7 truncations and point mutants generated in this study with a summary of the E3-ligase and microtubule-binding and -bundling activities of each recombinant protein. The gray box and asterisk denote the minimal microtubule-bundling domain defined as Xnf7$^{265–609}$.

(B) Immunofluorescent and negative-stain images of microtubule bundles assembled in the presence of 2 μM Xnf7$^{265–609}$. The 40× scale bar = 10 μm, the 7,500× scale bar = 1 μm, and the 30,000× scale bar = 200 nm.

(C) Addition of 5 μM Xnf7$^{1–432}$ (Xnf7ΔCTD) to spindle-assembly reactions dramatically disrupted microtubule organization and led to the formation of microtubule-associated and cytoplasmic clumps of Xnf7. In merged images, DNA is blue, tubulin is red, and Xnf7 is green. The scale bar = 10 μm.

(D) The top panels show Coomassie-stained gels of the recombinant full-length Xnf7 (WT) and Xnf7$^{265–609}$ used in the rescue experiments. The bottom panel shows an anti-Xnf7 western blot of extract samples from Δmock, ΔXnf7, and ΔXnf7+ 3 μM WT Xnf7 conditions. The recombinant Xnf7 was slightly smaller than the endogenous version of the protein. All the versions of recombinant Xnf7 used in these experiments were added at a final concentration of 3 μM to depleted extracts.

(E) Spindles were assembled in mock- and Xnf7-depleted extracts and challenged with 50 ng/ml nocodazole for 15 min before the number of collapsed/disorganized structures was tallied. Addition of either Xnf7 WT or Xnf7$^{265–609}$ to depleted extracts rescued the nocodazole sensitivity of ΔXnf7 spindles. Images show examples of spindle structures assembled in each condition. Tubulin is red and DNA is blue. The scale bar = 10 μm. The data were compiled from five separate depletion experiments, three of which included rescue conditions. The total numbers of structures counted were as follows: ΔMock and ΔXnf7 = 500, WT rescue = 200, and Xnf7$^{219–609}$ rescue = 300. Error bars are ± 1 standard deviation.

Microtubule-Associated Developmental Regulators

Xnf7 was initially characterized as a developmental regulator of dorsal-ventral patterning in the early *Xenopus* embryo. It is possible that Xnf7 is primarily involved in development but has been co-opted to fulfill a spindle role during mitosis by organizing microtubules. It is now evident that Xnf7 is not alone in this distinction. Developmental regulators such as APC, β-catenin, GSK-3β and dishevelled have all been shown to influence microtubule behavior [23–29]. It will be of significant interest to determine how the microtubule regulatory activities of these factors contribute to developmental patterning.

Xnf7 is retained in the cytoplasm of pre-MBT embryos, where it associates with microtubules throughout the early cell cycles [9, 17]. Perhaps this cytoplasmic retention of Xnf7 contributes to the proper organization of microtubules and/or affects the activity, level, or localization of other microtubule-associated proteins that contribute to early embryonic patterning. Interestingly, the E3-ligase activity of Xnf7 has recently been shown to be required to regulate the activity of another ubiquitin ligase, the anaphase-promoting complex (APC) [30]. Although this study indicated a role for Xnf7 in cell cycle regulation that could potentially be linked to spindle function, it does not preclude the participation of Xnf7 in developmental signaling pathways. In fact, targeting the E3-ligase activity of Xnf7 to microtubules may be an ideal strategy for spatially regulating the downstream targets of Xnf7 during both cell-cycle progression and development. In light of our work and the recent findings of Casaletto et al. [30], it will be extremely interesting to address the relative contributions of the different functional activities of Xnf7 and its downstream targets in dorsal-ventral patterning.

Xnf7 Family Members and Human Disease

A number of TRIM family members have been implicated in human diseases and developmental defects including the following: cancer (PML and RFP), mulibrey nanism (MUL), familial Mediterranean fever (PYRIN), Opitz syndrome (MID1), and HIV infection (TRIM5α) [31–33]. Whereas members share homology in the N-terminal tripartite regions, the C-terminal portion of TRIMs is divergent. The C-terminal SPRY domain of Xnf7 exhibits high homology with the C-terminal portions of several disease-linked TRIM family members including MID1 and TRIM5α [19, 32].

Interestingly, many mutations in MID1 that lead to Opitz syndrome (OS), a developmental disorder, affect the C-terminal SPRY domain and result in loss of proper microtubule localization and cytoplasmic aggregation of MID1 [20–22, 34]. In addition to its microtubule localization, MID1 has been shown to have ubiquitin-E3-ligase activity and has been proposed to indirectly regulate microtubule stability and organization by targeting phosphatase PP2A-C for degradation on microtubules potentially influencing MAP phosphorylation [35]. Perhaps MID1, like Xnf7, is itself a MAP that directly influences microtubule organization via bundling.

HIV emerged as a TRIM-linked disease when it was discovered that the protein TRIM5 mediates resistance to the human virus in rhesus monkey cells [33, 36, 37]. TRIM5α, the isoform that confers resistance, requires both its RING-finger and C-terminal SPRY domain to mediate the infection block [33]. Because the SPRY domain of Xnf7 and MID1 is required for proper microtubule localization, it will be interesting to investigate whether TRIM5α is also targeted to microtubules by its SPRY domain. Furthermore, it will be important to determine whether, like Xnf7 and MID1, TRIM5α exhibits RING-finger-dependent ubiquitin-E3-ligase activity and, if so, how this contributes to cellular HIV resistance.

Considering the similarities between Xnf7 and several TRIM family members, we envision that an understanding of Xnf7 may provide insight into TRIM-linked human diseases at the molecular, cellular, and developmental levels.

Supplemental Data

Supplemental data, including three movies, five supplemental figures, and Supplemental Experimental Procedures, are available at http://www.current-biology.com/cgi/content/full/15/19/1755/DC1/.

Acknowledgments

The authors would like to acknowledge L.D. Etkin for sending us the Xnf7 cDNA. We also thank O. Quintero, A. Wiedmann, U. Sheth, and A. Groen from the Woods Hole Physiology course for their help with the bundling and motility movies. Special thanks to both P. Budde and J. Banks for their guidance and thoughtful scientific discussions. Thank you to J. Brown for sharing reagents and ideas. We acknowledge both L. Coscoy and M. Deato for advice on E3-ligase assays. Thank you also to W. Clements and D. Kimmelman for preliminary studies and conversations on Xnf7 function in early development. We would also like to thank the Ran fan club, composed of Mike Blower, Petr Kalab, and Jon Soderholm, for thoughtful discussions and advice. Finally, we are extremely grateful to all members of the Heald, Weis, and Welch labs, past and present, for countless interesting scientific and nonscientific discussions. R.H. and K.W. are supported by the National Institutes of Health (GM65232).

Received: May 13, 2005
Revised: August 17, 2005
Accepted: August 18, 2005
Published: October 11, 2005

References

1. Mitchison, T.J., and Salmon, E.D. (2001). Mitosis: A history of division. Nat. Cell Biol. *3*, E17–E21.
2. El-Hodiri, H.M., Shou, W., and Etkin, L.D. (1997). xnf7 functions in dorsal-ventral patterning of the Xenopus embryo. Dev. Biol. *190*, 1–17.
3. Etkin, L.D., el-Hodiri, H.M., Nakamura, H., Wu, C.F., Shou, W., and Gong, S.G. (1997). Characterization and function of Xnf7 during early development of Xenopus. J. Cell. Physiol. *173*, 144–146.
4. Wittmann, T., Wilm, M., Karsenti, E., and Vernos, I. (2000). TPX2, a novel xenopus MAP involved in spindle pole organization. J. Cell Biol. *149*, 1405–1418.
5. Compton, D.A., and Cleveland, D.W. (1994). NuMA, a nuclear protein involved in mitosis and nuclear reformation. Curr. Opin. Cell Biol. *6*, 343–346.
6. Li, X., and Etkin, L.D. (1993). Xenopus nuclear factor 7 (xnf7) possesses an NLS that functions efficiently in both oocytes and embryos. J. Cell Sci. *105*, 389–395.
7. Reymond, A., Meroni, G., Fantozzi, A., Merla, G., Cairo, S., Luzi, L., Riganelli, D., Zanaria, E., Messali, S., Cainarca, S., et al. (2001). The tripartite motif family identifies cell compartments. EMBO J. *20*, 2140–2151.
8. Jensen, K., Shiels, C., and Freemont, P.S. (2001). PML protein isoforms and the RBCC/TRIM motif. Oncogene *20*, 7223–7233.
9. Li, X., Shou, W., Kloc, M., Reddy, B.A., and Etkin, L.D. (1994). Cytoplasmic retention of Xenopus nuclear factor 7 before the mid blastula transition uses a unique anchoring mechanism involving a retention domain and several phosphorylation sites. J. Cell Biol. *124*, 7–17.
10. Miller, M., Reddy, B.A., Kloc, M., Li, X.X., Dreyer, C., and Etkin, L.D. (1991). The nuclear-cytoplasmic distribution of the Xenopus nuclear factor, xnf7, coincides with its state of phosphorylation during early development. Development *113*, 569–575.
11. Bellini, M., Lacroix, J.C., and Gall, J.G. (1995). A zinc-binding domain is required for targeting the maternal nuclear protein PwA33 to lampbrush chromosome loops. J. Cell Biol. *131*, 563–570.
12. Bellini, M., Lacroix, J.C., and Gall, J.G. (1993). A putative zinc-binding protein on lampbrush chromosome loops. EMBO J. *12*, 107–114.
13. Andersen, S.S.L., Ashford, A.J., Tournebize, R., Gavet, O., Sobel, A., Hyman, A.A., and Karsenti, E. (1997). Mitotic chromatin regulates phosphorylation of Stathmin/Op18. Nature *389*, 640–643.
14. Belmont, L.D., and Mitchison, T.J. (1996). Identification of a protein that interacts with tubulin dimers and increases the catastrophe rate of microtubules. Cell *84*, 623–631.
15. Budde, P.P., Kumagai, A., Dunphy, W.G., and Heald, R. (2001). Regulation of op18 during spindle assembly in Xenopus egg extracts. J. Cell Biol. *153*, 149–158.
16. Cheeseman, I.M., Brew, C., Wolyniak, M., Desai, A., Anderson, S., Muster, N., Yates, J.R., Huffaker, T.C., Drubin, D.G., and Barnes, G. (2001). Implication of a novel multiprotein Dam1p complex in outer kinetochore function. J. Cell Biol. *155*, 1137–1145.
17. Shou, W., Li, X., Wu, C., Cao, T., Kuang, J., Che, S., and Etkin, L.D. (1996). Finely tuned regulation of cytoplasmic retention of Xenopus nuclear factor 7 by phosphorylation of individual threonine residues. Mol. Cell. Biol. *16*, 990–997.
18. Stein, P.A., Toret, C.P., Salic, A.N., Rolls, M.M., and Rapoport, T.A. (2002). A novel centrosome-associated protein with affinity for microtubules. J. Cell Sci. *115*, 3389–3402.
19. Henry, J., Mather, I.H., McDermott, M.F., and Pontarotti, P. (1998). B30.2-like domain proteins: Update and new insights into a rapidly expanding family of proteins. Mol. Biol. Evol. *15*, 1696–1705.
20. Gaudenz, K., Roessler, E., Quaderi, N., Franco, B., Feldman, G., Gasser, D.L., Wittwer, B., Horst, J., Montini, E., Opitz, J.M., et al. (1998). Opitz G/BBB syndrome in Xp22: Mutations in the MID1 gene cluster in the carboxy-terminal domain. Am. J. Hum. Genet. *63*, 703–710.
21. Cox, T.C., Allen, L.R., Cox, L.L., Hopwood, B., Goodwin, B., Haan, E., and Suthers, G.K. (2000). New mutations in MID1 provide support for loss of function as the cause of X-linked Opitz syndrome. Hum. Mol. Genet. *9*, 2553–2562.
22. Schweiger, S., Foerster, J., Lehmann, T., Suckow, V., Muller, Y.A., Walter, G., Davies, T., Porter, H., van Bokhoven, H., Lunt, P.W., et al. (1999). The Opitz syndrome gene product, MID1, associates with microtubules. Proc. Natl. Acad. Sci. USA *96*, 2794–2799.

23. Zumbrunn, J., Kinoshita, K., Hyman, A.A., and Nathke, I.S. (2001). Binding of the adenomatous polyposis coli protein to microtubules increases microtubule stability and is regulated by GSK3 beta phosphorylation. Curr. Biol. *11*, 44–49.
24. Krylova, O., Messenger, M.J., and Salinas, P.C. (2000). Dishevelled-1 regulates microtubule stability: A new function mediated by glycogen synthase kinase-3beta. J. Cell Biol. *151*, 83–94.
25. Wakefield, J.G., Stephens, D.J., and Tavare, J.M. (2003). A role for glycogen synthase kinase-3 in mitotic spindle dynamics and chromosome alignment. J. Cell Sci. *116*, 637–646.
26. Dikovskaya, D., Newton, I.P., and Nathke, I.S. (2004). The adenomatous polyposis coli protein is required for the formation of robust spindles formed in CSF Xenopus extracts. Mol. Biol. Cell *15*, 2978–2991.
27. Mogensen, M.M., Tucker, J.B., Mackie, J.B., Prescott, A.R., and Nathke, I.S. (2002). The adenomatous polyposis coli protein unambiguously localizes to microtubule plus ends and is involved in establishing parallel arrays of microtubule bundles in highly polarized epithelial cells. J. Cell Biol. *157*, 1041–1048.
28. Kaplan, K.B., Burds, A.A., Swedlow, J.R., Bekir, S.S., Sorger, P.K., and Nathke, I.S. (2001). A role for the Adenomatous Polyposis Coli protein in chromosome segregation. Nat. Cell Biol. *3*, 429–432.
29. Ligon, L.A., Karki, S., Tokito, M., and Holzbaur, E.L. (2001). Dynein binds to beta-catenin and may tether microtubules at adherens junctions. Nat. Cell Biol. *3*, 913–917.
30. Casaletto, J.B., Nutt, L.K., Wu, Q., Moore, J.D., Etkin, L.D., Jackson, P.K., Hunt, T., and Kornbluth, S. (2005). Inhibition of the anaphase-promoting complex by the Xnf7 ubiquitin ligase. J. Cell Biol. *169*, 61–71.
31. Quaderi, N.A., Schweiger, S., Gaudenz, K., Franco, B., Rugarli, E.I., Berger, W., Feldman, G.J., Volta, M., Andolfi, G., Gilgenkrantz, S., et al. (1997). Opitz G/BBB syndrome, a defect of midline development, is due to mutations in a new RING finger gene on Xp22. Nat. Genet. *17*, 285–291.
32. Torok, M., and Etkin, L.D. (2001). Two B or not two B? Overview of the rapidly expanding B-box family of proteins. Differentiation *67*, 63–71.
33. Stremlau, M., Owens, C.M., Perron, M.J., Kiessling, M., Autissier, P., and Sodroski, J. (2004). The cytoplasmic body component TRIM5alpha restricts HIV-1 infection in Old World monkeys. Nature *427*, 848–853.
34. Cainarca, S., Messali, S., Ballabio, A., and Meroni, G. (1999). Functional characterization of the Opitz syndrome gene product (midin): Evidence for homodimerization and association with microtubules throughout the cell cycle. Hum. Mol. Genet. *8*, 1387–1396.
35. Trockenbacher, A., Suckow, V., Foerster, J., Winter, J., Krauss, S., Ropers, H.H., Schneider, R., and Schweiger, S. (2001). MID1, mutated in Opitz syndrome, encodes an ubiquitin ligase that targets phosphatase 2A for degradation. Nat. Genet. *29*, 287–294.
36. Yap, M.W., Nisole, S., and Stoye, J.P. (2005). A single amino acid change in the SPRY domain of human Trim5alpha leads to HIV-1 restriction. Curr. Biol. *15*, 73–78.
37. Yap, M.W., Nisole, S., Lynch, C., and Stoye, J.P. (2004). Trim5alpha protein restricts both HIV-1 and murine leukemia virus. Proc. Natl. Acad. Sci. USA *101*, 10786–10791.